PERGAMON

International Journal of Solids and Structures 37 (2000) 5561–5578

INTERNATIONAL JOURNAL OF SOLIDS and STRUCTURES

www.elsevier.com/locate/ijsolstr

General solutions for thermopiezoelectrics with various holes under thermal loading

Qing-Hua Qin

Department of Mechanical Engineering, University of Sydney, Sydney, NSW 2006, Australia

Received 3 August 1999

Abstract

The thermoelectroelastic problems for a hole of various shapes embedded in an infinite matrix are considered in this paper. Using Stroh's formalism and the technique of conformal mapping, a unified solution is obtained in closed-form for an infinite thermopiezoelectric plate with various holes induced by thermal loads. The loads may be uniform remote heat flow, point heat source and temperature discontinuity. Further a detailed discussion on the critical points for the mapping function of a piezoelectric plate with polygonal holes is presented and the study shows that the transformation is nonsingle-valued. A simple approach is given to treat such a situation. As an application of the proposed solutions, a system of singular integral equations for the unknown temperature discontinuity and the dislocation of elastic displacement and electric potential defined on crack faces is developed and solved numerically. Numerical results are presented to illustrate the application of the proposed formulation.

Keywords: Crack; Piezoelectric; Thermomechanical voids; Integral equation

1. Introduction

Studies on the stress concentration induced by holes or cracks in composite materials has been a topic of considerable research, and many useful results and conclusions have been made during the past decades (Kachanov et al., 1994). Of various holes the elliptic shape has evoked the most interest among researchers for isothermal problems because of its flexibility to include the other special shapes such as circles or cracks. However, the optimization process on a class of hole shapes showed that the optimized hole is not necessary an ellipse (Dhir, 1981). Thus the study on thermal stress induced by holes differing from ellipse is also of engineering importance. For isotropic materials, Evan-Iwanowski (1956) used the

E-mail address: qin@mech.eng.usyd.edu.au (Q.-H. Qin).

0020-7683/00/$ - see front matter
PII: S0020-7683(99)00225-5

complex variable approach to derive the stress solutions for an infinite isotropic plate with a triangular inlay. Florence and Goodier (1960) studied the thermal stress for an isotropic medium containing an insulated oval hole. Based on the complex variable method, Chen (1967) studied the orthotropic medium with a circular or elliptic hole, and obtained a complex form solution for the hoop stress around the hole. Zimmerman (1986) studied the compressibility of holes by way of conformal mapping of a hole onto a unit circle. Kachanov et al. (1994) developed a unified description concerning both cavities and cracks. For orthotropic plate with rectangular openings, work has been done by Jong (1981) and Rajaiah and Naik (1983). Their results were based on the solutions given by Lekhnitskii (1968), which are only approximate solutions due to the mathematical difficulties involved. Based on the Stroh formalism and complex conformal mapping, Hwu (1990) obtained the stress fields for an anisotropic elastic plate with an hole of various shapes subjected to remote uniform mechanical loading. For plane piezoelectric material without considering thermal effect, Sosa and Khutoryansky (1996) obtained an analytical solution of piezoelectricity with an elliptic hole. Chung and Ting (1996) also presented a general solution for piezoelectric plate with an elliptic inclusion. Recently, Hwu and Yen (1991) obtained the Green's functions satisfying traction-free boundary conditions around an elliptic hole of anisotropic materials using Stroh's formalism. Ting (1992) in his work presented the Green's functions for half-space and bimaterials of anisotropic plates. Later, Yen et al. (1995) and Ting (1996) obtained Green's functions for a line force and a line dislocation located outside, inside or on the interface of an elliptic inclusion of general anisotropic elastic materials. In the literature, however, there is very little work concerned with the thermoelastic Green's function. Sturla and Barber (1988) obtained a solution of thermoelastic Green's functions for two-dimensional problem of an infinite elastic plate subjected to a temperature discontinuity along the axis $x_2 = 0$. Qin et al. (1999) in their work presented thermoelectroelastic Green's functions for bimaterial.

Besides the fundamental academic interest, the determination of appropriate mapping functions in hole problems is also considerable importance. It is relatively simple in the case of isotropic materials because only a single mapping function is required. The conformal-mapping becomes considerably difficult in the case of piezoelectric materials, since it requires finding four distinct mapping functions which transform the complex parameter regions onto the exterior of a unit circle. For general anisotropic materials, Lekhnitskii (1968) presented a conformal-mapping scheme to solve a number of problems on elliptical holes and inclusions. By combining the boundary-perturbation approach and Lekhnitskii's conformal mapping scheme, Gao (1992) obtained a first-order perturbation solution for anisotropic elastic solids with a smooth polygonal hole. To make it clear in what cases the conformal mapping scheme can be applied to general boundary value problem, Wang and Tarn (1993) investigated the conditions under which the conformal mapping is possible. Their study indicated that the conformal mapping in the entire region outside the unit circles possible only for elliptic contour or for anisotropy of a special kind. Hwu (1992) in his study on anisotropic media revealed that the mapping function $z_k = a(a_{1k}\zeta_k + a_{2k}\zeta_k^{-1} + e_{m1}a_{3k}\zeta_k^{m} + e_{m1}a_{4k}\zeta_k^{-m})$ will map the contour of a polygonal hole on to a circle in the ζ-plane, and there will be m distinct ζ_k located outside the unit circle. The problem is that which one should we take. Hwu (1992) in his study chose one nearest $|\zeta| = 1$ as the mapping point, but no explanation can be found in his paper. This is the motivation that we try to explain the reasons why the one nearest $|\zeta| = 1$ should be chosen in this paper.

In view of the above analysis, the purpose of this paper is to present a unified thermoelectroelastic solution for an infinite thermopiezoelectric plate with various openings induced by thermal loads. The load may be uniform remote heat flow, point heat source and temperature discontinuity. The solutions for the later two cases are often called as Green's function, which has a wide application in boundary element technique and other numerical analysis. The Green's function developed is used to derive the thermoelectroelastic solution for the interaction between a crack and a hole embedded in an infinite

thermopiezoelectric plate. Numerical results for SED intensity factors are presented to verify the effectiveness of the proposed formulation.

2. Preliminary formulations

2.1. Stroh formulation for linear thermopiezoelectric solid

Consider a linear piezoelectric solid where all fields are the function of x_1 and x_2 only. Cartesian coordinate system (x_1, x_2, x_3) is used for the description of all field quantities and, boldfaced symbols stand for either column vectors or matrices, depending on whether lower case or upper case is used. For stationary behaviour in the absence of body heat source, free electric charge and body forces, the Stroh formulation of linear thermoelectroelasticity can be found in Mindlin (1974) and Barnett and Lothe (1975):

$$T = g'(z_t) + \overline{g'(z_t)} \tag{1a}$$

$$\vartheta = -ikg'(z_t) + ik\overline{g'(z_t)} \tag{1b}$$

$$h_1 = -\vartheta_{,2} \qquad h_2 = \vartheta_{,1} \tag{1c}$$

$$\mathbf{u} = \mathbf{AF(z)q} + \mathbf{c}g(z_t) + \overline{\mathbf{AF(z)q}} + \overline{\mathbf{c}g(z_t)} \tag{1d}$$

$$\boldsymbol{\phi} = \mathbf{BF(z)q} + \mathbf{d}g(z_t) + \overline{\mathbf{BF(z)q}} + \overline{\mathbf{d}g(z_t)} \tag{1e}$$

$$\boldsymbol{\Pi}_1 = -\boldsymbol{\phi}_{,2}, \qquad \boldsymbol{\Pi}_2 = \boldsymbol{\phi}_{,1} \tag{1f}$$

with

$$\mathbf{F(z)} = \mathrm{diag}\big[f(z_1) \quad f(z_2) \quad f(z_3) \quad f(z_4)\big]$$

$$z_t = x_1 + \tau x_2, \qquad z_i = x_1 + p_i x_2 \tag{2}$$

where overbar denotes the complex conjugate, a prime represents the differentiation with respect to the argument, $\mathbf{q}$ is a constant vector to be determined by the boundary conditions, $\mathbf{u} = \{u_1\ u_2\ u_3\ \varphi\}^{\mathrm{T}}$, $\boldsymbol{\Pi}_j = \{\sigma_{1j}\ \sigma_{2j}\ \sigma_{3j}\ D_j\}^{\mathrm{T}}$, $j = 1,2$; $i = \sqrt{-1}$, $k = \sqrt{k_{11}k_{22} - k_{12}^2}$, k_{ij} are the coefficients of heat conduction, u_i and φ are the elastic displacement and electric potential (EDEP), T, h_i, σ_{ij} and D_i are temperature, heat flow, stress and electric displacement, τ and p_i are the heat and electroelastic eigenvalues of the materials whose imaginary parts are positive, ϑ and ϕ are known as heat-flow function and SED function (Qin, 1998), $f(z_i)$ and $g(z_t)$ are arbitrary functions with complex arguments z_i and z_t, respectively, $\mathbf{A}$, $\mathbf{B}$, $\mathbf{c}$ and $\mathbf{d}$ are well-defined in the literature (see Qin et al., 1999 for example).

2.2. One-to-one mapping

The contour of the hole used, say Γ (see Fig. 1), in this paper is represented by (Hwu, 1990)

$$x_1 = a(\cos\psi + \gamma e_{ml}\cos m\psi), \qquad x_2 = a(e\sin\psi - \gamma e_{ml}\sin m\psi) \tag{3}$$

where $e_{ij} = 1$ if $i \neq j$; $e_{ij} = 0$ if $i = j$, $0 < e \leq 1$, m is an integer and have same value for subscript and for the argument of functions. By an appropriate selection of the parameters e, m and γ, we can obtain various special kinds of holes, such as ellipse ($m = 1$), circle ($m = e = 1$), triangular ($m = 2$), square ($m = 3$) and pentagon ($m = 4$). Since the conformal mapping is a fundamental tool used to find the solution of hole problem, the transformation (Hwu, 1990)

$$z_k = a\left(a_{1k}\zeta_k + a_{2k}\zeta_k^{-1} + e_{ml}a_{3k}\zeta_k^{m} + e_{ml}a_{4k}\zeta_k^{-m}\right) \tag{4}$$

in which

$$a_{1k} = \frac{1 - ip_k e}{2}, \quad a_{2k} = \frac{1 + ip_k e}{2}, \quad a_{3k} = \frac{\gamma(1 + ip_k e)}{2}, \quad a_{4k} = \frac{\gamma(1 - ip_k e)}{2} \tag{5}$$

will be used to map the contour of the hole on to a unit circle in the ζ-plane. For a particular value of z_k, there exist $2m$ roots for ζ_k in Eq. (4). Numerical study on Eq.(4) shows that half of the roots are located outside the unit circle, and the remaining are inside the unit circle. Thus, the transformation (4) will be single-valued for $m = 1$ (ellipse) since only one root locates outside the unit circle. For $m > 1$, however, the transformation (4) is multi-valued as there are m roots located outside the unit circle. The question is which one should be chosen. To fix this, some numerical investigation has been performed and the typical results are listed in Tables 1–3 for $a = e = 1$and $\gamma = 0.1$. In these tables, $p_k = -0.2291853 + 1.003833i$, which is one of the eigenvalues of material $BaTiO_3$ used in Section 5, $|\zeta|^2 = \zeta\bar{\zeta}$, ζ_{ki} is the ith root of ζ_k for Eq. (4). It is found from the tables that the magnitudes among the m-roots are obviously different from each other. In order to show which mapping points can provide correct solutions some numerical results are presented in Section 5. The numerical results show the root, say ζ_k^*, whose magnitude has a minimum value among the m-roots, can provide acceptable results. So we will chose ζ_k^* as the solution for Eq. (4) in our analysis. Hence, the entire z_k-plane is now mapped

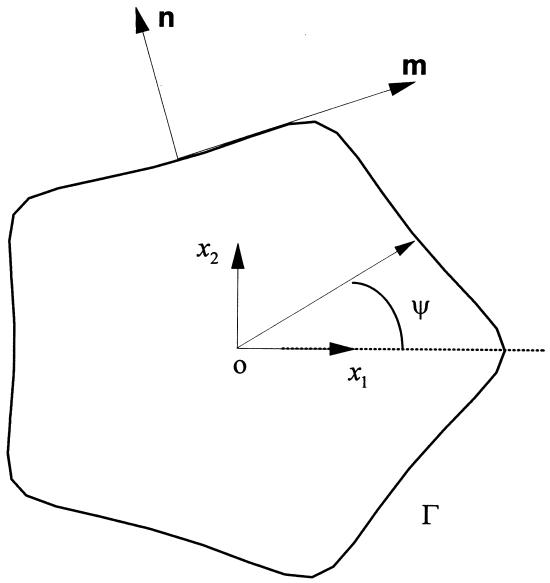

Fig. 1. Geometry of a particular hole ($a = 1$, $e = 1$, $m = 4$, $\gamma = 0.1$).

Table 1
The properties of solution ξ_{km} for $j = 2$

z_k	$5 + 5p_k$	$-5 + 5p_k$	$-5 - 5p_k$	$5 - 5p_k$
ξ_{k1}	$7.51 - 91.75i$	$16.35 - 92.73i$	$16.30 - 82.84i$	$5.156 - 81.586i$
$\lvert\xi_{k1}\rvert$	92.06	94.16	84.43	81.74
ξ_{k2}	$3.97 + 4.52i$	$-4.885 + 5.4757i$	$-4.85 - 4.41i$	$6.294 - 5.65i$
$\lvert\xi_{k2}\rvert$	6.016	7.338	6.555	8.458

onto part of the ζ_k-plane with a one-to-one transformation. Moreover, it is interesting to see from Tables 1–3 that the real and imaginary parts of ζ_k^* always keep the same symbol as those of z_k, i.e., $\mathrm{Sign}[\mathrm{Im}(z_k)] = \mathrm{Sign}[\mathrm{Im}(\zeta_k^*)]$ and $\mathrm{Sign}[\mathrm{Re}(z_k)] = \mathrm{Sign}[\mathrm{Re}(\zeta_k^*)]$, where

$$\mathrm{Sign}(x) = \begin{cases} 1 & \text{if } x > 0 \\ 0 & \text{if } x = 0 \\ -1 & \text{if } x < 0 \end{cases} \tag{6}$$

which means that ζ_k^* and z_k are always situated in the same quadrant of a rectangular coordinates system.

3. Green's function for traction-free hole problem

Consider an infinite piezoelectric plate contain a hole subjected to thermal loading. If the hole is thermal-insulated, traction- and charge-free along the hole boundary, the boundary conditions at the rim of the hole can be written as

$$\vartheta = \boldsymbol{\phi} = 0 \tag{7}$$

here the following relations has been used (Hwu and Yen, 1993)

$$h_n = \vartheta_{,s}, \qquad \mathbf{t}_n = \boldsymbol{\phi}_{,s} \tag{8}$$

where n is the normal direction of the hole, s is the arc length measured along the hole boundary, $\mathbf{t}_n$ represents surface traction vector.

3.1. General solution for thermal field

Based on the one-to-one mapping described above and the concept of perturbation given by Stagni (1982), the general solution for temperature and heat-flow function can be assumed in the form (Hwu

Table 2
The properties of solution ζ_{km} for $j = 3$

z_k	$5 + 5p_k$	$-5 + 5p_k$	$-5 - 5p_k$	$5 - 5p_k$
ζ_{k1}	$6.02 - 8.63i$	$8.96 - 8.07i$	$9.39 - 5.05i$	$-8.96 + 8.07i$
$\lvert\zeta_{k1}\rvert$	10.52	12.06	10.66	12.06
ζ_{k2}	$-9.39 + 5.05i$	$-7.73 + 0.784i$	$-6.02 + 8.63i$	$7.73 - 0.784i$
$\lvert\zeta_{k2}\rvert$	10.66	7.770	10.52	7.770
ζ_{k2}	$3.38 + 3.60i$	$-1.221 + 7.274i$	$-3.38 - 3.60i$	$1.221 - 7.274i$
$\lvert\zeta_{k2}\rvert$	4.938	7.376	4.938	7.376

and Yen, 1993)

$$T = 2\mathrm{Re}\big[g'(z_t)\big] = 2\mathrm{Re}\big[f_0(\zeta_t) + f_1(\zeta_t)\big] \tag{9}$$

$$\vartheta = -2\mathrm{Re}\big[ikg'(z_t)\big] = -2\mathrm{Re}\big[ikf_0(\zeta_t) + ikf_1(\zeta_t)\big] \tag{10}$$

where f_0 represents the solution associated with the unperturbed thermal field and f_1 is the function corresponding to perturbed field of the plate.

For a given loading condition, the function f_0 can be obtained easily since it is related to the solution of homogeneous media. When an infinite plate subjected to a line temperature discontinuity T_0 and a line heat source h^* both located at $\hat{z}_t(= x_{10} + \tau x_{20})$, the function f_0 can be chosen in the form (Sturla and Barber, 1988)

$$f_0(\zeta_t) = q_0 \ln\big(\zeta_t - \zeta_t^*\big) \tag{11}$$

where ζ_t and ζ_t^* are related to the complex arguments z_t and $\hat{z}_t$ through the transformation function (4), and q_0 is a complex constant which can be determined from the conditions

$$\int_C \mathrm{d}T = T_0 \quad \text{and} \int_C \mathrm{d}\vartheta = -h^*, \text{ for any closed curve } C \text{ enclosing the point } \zeta_t^* \tag{12}$$

The substitution of Eq. (11) into Eqs. (12) yields

$$q_0 = \frac{T_0}{4\pi i} - \frac{h^*}{4\pi k} \tag{13}$$

When the thermal load is uniform remote heat flux $\mathbf{h}(h_{10}, h_{20})$ the function f_0 may be assumed as (Hwu and Yen, 1993)

$$f_0(\zeta_t) = q_0^* z_t \tag{14}$$

the infinite condition provides

$$q_0^* = \frac{h_{10} + h_{20}\bar{\tau}}{ik(\tau - \bar{\tau})} \tag{15}$$

Thus, the boundary condition (7) requires that

Table 3
The properties of solution ξ_{km} for $j = 4$

z_k	$5 + 5p_k$	$-5 + 5p_k$	$-5 - 5p_k$	$5 - 5p_k$
ζ_{k1}	$-4.69 - 3.22i$	$4.58 - 2.98i$	$5.23 - 1.53i$	$-5.31 - 1.88i$
$\lvert\zeta_{k1}\rvert$	5.689	5.464	5.449	5.633
ξ_{k2}	$-2.02 + 4.43i$	$1.94 + 4.68i$	$-4.43 - 0.16i$	$4.78 + 0.30i$
$\lvert\zeta_{k2}\rvert$	4.869	5.066	4.433	4.789
ζ_{k3}	$3.71 - 3.61i$	$-3.52 - 4.15i$	$0.436 + 5.58i$	$-0.94 + 5.75i$
$\lvert\zeta_{k3}\rvert$	5.177	5.442	5.597	5.826
ζ_{k4}	$3.01 + 2.41i$	$-3.49 + 2.45i$	$-1.255 - 3.90i$	$1.46 - 4.15i$
$\lvert\zeta_{k4}\rvert$	3.856	4.264	4.097	4.399

$$f_1(\zeta_t) = \bar{q}_0 \ln\left(\zeta_t^{-1} - \bar{\zeta}_t^*\right) \quad \text{or} \quad f_1(\zeta_t) = a\bar{q}_0^*\left(\bar{a}_{1\tau}\zeta_t^{-1} + \bar{a}_{2\tau}\zeta_t + \bar{a}_{3\tau}\zeta_t^{-m} + \bar{a}_{4\tau}\zeta_t^m\right) \tag{16}$$

where

$$a_{1\tau} = \frac{1 - i\tau e}{2}, \qquad a_{2\tau} = \frac{1 + i\tau e}{2} \tag{17}$$

$$a_{3\tau} = \frac{\gamma(1 + i\tau e)}{2}, \qquad a_{4\tau} = \frac{\gamma(1 - i\tau e)}{2} \tag{18}$$

The function g in Eq. (9) can, thus, be obtained by integrating the functions f_0 and f_1 with respect to z_t, which leads to

$$g(z_t) = aa_{1\tau}\left[q_0 F_1(\zeta_t, \zeta_t^*) + \bar{q}_0 F_2\left(\zeta_t^{-1}, \bar{\zeta}_t^*\right)\right] + a_{2\tau}\left[q_0 F_2(\zeta_t, \zeta_t^*) + \bar{q}_0 F_1\left(\zeta_t^{-1}, \bar{\zeta}_t^*\right)\right]$$

$$+ae_{j1}a_{3\tau}\left[q_0 F_3(\zeta_t, \zeta_t^*) + \bar{q}_0 F_4\left(\zeta_t^{-1}, \bar{\zeta}_t^*\right)\right] + a_{4\tau}\left[q_0 F_4(\zeta_t, \zeta_t^*) + \bar{q}_0 F_3\left(\zeta_t^{-1}, \bar{\zeta}_t^*\right)\right] \tag{19}$$

where

$$F_1(\zeta_t, \zeta_t^*) = (\zeta_t - \zeta_t^*)\left[\ln(\zeta_t - \zeta_t^*) - 1\right] \tag{20}$$

$$F_2(\zeta_t, \zeta_t^*) = \left(\zeta_t^{-1} - \zeta_t^{*-1}\right)\ln(\zeta_t - \zeta_t^*) + \zeta_t^{*-1}\ln\zeta_t, \tag{21}$$

$$F_3(\zeta_t, \zeta_t^*) = (\zeta_t^m - \zeta_t^{*m})\ln(\zeta_t - \zeta_t^*) - \zeta_t^{*m}\sum_{n=1}^{m}\frac{1}{n}\left(\frac{\zeta_t}{\zeta_t^*}\right)^n, \tag{22}$$

$$F_4(\zeta_t, \zeta_t^*) = (\zeta_t^{-m} - \zeta_t^{*-m})\ln(\zeta_t - \zeta_t^*) + \zeta_t^{*-m}\ln\zeta_t - \zeta_t^{*-m}\sum_{n=1}^{m-1}\frac{1}{n}\left(\frac{\zeta_t^*}{\zeta_t}\right)^n, \tag{23}$$

The expression of g corresponding to the loading case q_0^* can be also obtained similarly.

3.2. General solution for electroelastic field

From Eqs. (1d) and (1e), the particular solution of electroelastic field induced by thermal loading can be written as

$$\mathbf{u}_{\mathrm{p}} = 2\mathrm{Re}\left[\mathbf{c}g(z_t)\right], \qquad \boldsymbol{\phi}_{\mathrm{p}} = 2\mathrm{Re}\left[\mathbf{d}g(z_t)\right] \tag{24}$$

where subscript 'p' refers to particular solution.

The particular solutions (24) do not, generally, satisfy the boundary condition (7) along the hole boundary. We, therefore, need to seek a corrective isothermal solution for a given problem when superposed on the particular thermoelectroelastic solution the surface conditions (7) will be satisfied. Owing to the fact that $f(z_k)$ and $g(z_t)$ have the same order to affect the stress and electric displacement in Eqs. (1d) and (1e), possible function forms come from the partition of $g(z_t)$. They are

$$f_1(z_k) = a\Big[q_0F_1\big(\zeta_k, \zeta_t^*\big) + q_0F_2\big(\zeta_k, \zeta_t^*\big) + \bar{q}_0F_1\Big(\zeta_k^{-1}, \bar{\zeta}_t^*\Big) + \bar{q}_0F_2\Big(\zeta_k^{-1}, \bar{\zeta}_t^*\Big)\Big]/2$$

$$+e_{j1}a\gamma\Big[q_0F_3\big(\zeta_k, \zeta_t^*\big) + q_0F_4\big(\zeta_k, \zeta_t^*\big) + \bar{q}_0F_3\Big(\zeta_k^{-1}, \bar{\zeta}_t^*\Big) - \bar{q}_0F_4\Big(\zeta_k^{-1}, \zeta_t^*\Big)\Big]/2,$$

$$f_2(z_k) = ip_kae\Big[-q_0F_1\big(\zeta_k, \zeta_t^*\big)q_0F_2\big(\zeta_k, \zeta_t^*\big) + \bar{q}_0F_1\Big(\zeta_k^{-1}, \bar{\zeta}_t^*\Big) - \bar{q}_0 - F_2\Big(\zeta_k^{-1}, \bar{\zeta}_t^*\Big)\Big]/2$$

$$+ie_{j1}p_kae\gamma\Big[q_0F_3\big(\zeta_k, \zeta_t^*\big) - q_0F_4\big(\zeta_k, \zeta_t^*\big) - \bar{q}_0F_3\Big(\zeta_k^{-1}, \bar{\zeta}_t^*\Big) + \bar{q}_0F_4\Big(\zeta_k^{-1}, \bar{\zeta}_t^*\Big)\Big]/2 \tag{25}$$

where the subscripts 1 and 2 are the indices for the different possible functions.

The Green's functions for the electroelastic fields can thus be chosen as

$$\mathbf{u} = 2\mathrm{Re}\left\{\sum_{k=1}^{2}\big[\mathbf{A}\mathbf{F}_k(\mathbf{z})\mathbf{q}_k\big] + \mathbf{c}g(z_t)\right\} \tag{26a}$$

$$\boldsymbol{\phi} = 2\mathrm{Re}\left\{\sum_{k=1}^{2}\big[\mathbf{B}\mathbf{F}_k(\mathbf{z})\mathbf{q}_k\big] + \mathbf{d}g(z_t)\right\} \tag{26b}$$

Substitution of Eq. (25) into Eq. (26b), later into Eq. (7), leads to

$$\mathbf{q}_1 = -\mathbf{B}^{-1}\bar{\mathbf{d}}, \qquad \mathbf{q}_2 = -\mathbf{P}^{-1}\mathbf{B}^{-1}\bar{\mathbf{d}}\bar{\tau} \tag{27}$$

Substituting Eq. (27) into Eq. (26), the Green's functions can, then, be written as

$$\mathbf{u} = 2\mathrm{Re}\Big\{-\mathbf{A}\big[\mathbf{F}_1(\mathbf{z}) + \mathbf{F}_2(\mathbf{z})\mathbf{P}^{-1}\bar{\tau}\big]\mathbf{B}^{-1}\bar{\mathbf{d}} + \mathbf{c}g(z_t)\Big\} \tag{28}$$

$$\boldsymbol{\phi} = 2\mathrm{Re}\Big\{-\mathbf{B}\big[\mathbf{F}_1(\mathbf{z}) + \mathbf{F}_2(\mathbf{z})\mathbf{P}^{-1}\bar{\tau}\big]\mathbf{B}^{-1}\bar{\mathbf{d}} + \mathbf{d}g(z_t)\Big\} \tag{29}$$

Solutions for loading case q_0^* can be also obtained similarly, and we can prove that they are the same as those given by Qin et al. (1999) if we neglect a uniform heat flow in the solution domain.

4. Interaction between a crack and a hole

To illustrate the application of the proposed Green's functions, consider an infinite piezoelectric plate with a crack of length of $2c$ and a hole of various shapes subjected to heat flux h_0 on the crack faces. The central point of the crack is denoted by $z_k^0(= x_{10} + p_k x_{20})$ and its orientation angle is denoted by α. The geometry of the configuration of the crack-hole system is shown in Fig. 2. The orientation of the crack may be arbitrary. The mathematical statement of this problem can be stated more precisely as follows

$$h_n = h_0, \text{ on crack faces} \tag{30a}$$

$$\boldsymbol{\Pi}_n = 0 \qquad \text{on crack faces} \tag{30b}$$

$$h_n = \mathbf{t}_n = 0 \qquad \text{on the hole boundary} \tag{31}$$

$$h_i = \boldsymbol{\Pi}_i = 0 \quad i = 1, 2; \text{ at infinity} \tag{32}$$

The boundary conditions (30), can be satisfied by redefining the discrete Green's functions q_0 in Eq. (19) in terms of distributing Green's functions$q_0(\xi)$ defined along the crack line, $z_t = z_t^0 + \eta z_t^*$, $\hat{z}_t = z_t^0 + \xi z_t^*$, where $z_t^0 = x_{10} + \tau x_{20}$, $z_t^* = \cos\alpha + \tau \sin\alpha$. In this case, the load parameter q_0 appearing in Section 3 should be taken as $T_0(\xi/4\Pi i)$. Enforcing the satisfaction of the applied heat flux conditions on the crack faces, a singular integral equation for the Green's function is obtained as

$$\frac{1}{\pi}\mathrm{Re}\left[\int_{-c}^{c}\left[\frac{1}{\eta-\xi} + K_0(\eta, \xi)\right]T_0(\xi)\,\mathrm{d}\xi\right] = -\frac{2h_0}{k} \tag{33}$$

where K_0 is Holder-continuous along $-c \le \xi \le c$ and is given by

$$K_0(\eta, \xi) = -z_t^*\left[\frac{\partial z_\mathrm{p}/\partial\zeta_t}{z_\mathrm{p}} - \frac{1}{\zeta_t\left(1-\xi_t\bar{\zeta}_t^*\right)}\right]\frac{\partial\zeta_t}{\partial z_t} \tag{34}$$

where

$$z_\mathrm{p} = a_{1\tau} - \frac{a_{2\tau}}{\zeta_t\zeta_t^*} + \left(a_{3\tau} - \frac{a_{4\tau}}{\zeta_t^m\zeta_t^{*m}}\right)\sum_{k=0}^{m-1}\zeta_t^k\zeta_t^{*m-k-1} \tag{35}$$

During the derivation of Eq. (33), the following relation has been employed

$$\ln\left(\zeta_t - \zeta_t^*\right) = \ln(z_t - \hat{z}_t) - \ln z_\mathrm{p} \tag{36}$$

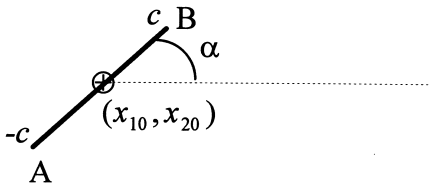

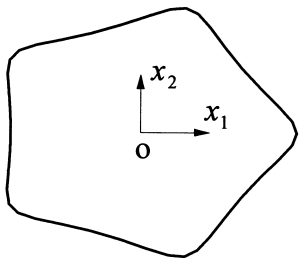

Fig. 2. Geometry of the crack-hole system.

For a single-valued temperature around a closed contour surrounding the whole crack, the following auxiliary condition has to be satisfied

$$\int_{-c}^{c} T_0(\xi)\,\mathrm{d}\xi = 0 \tag{37}$$

The singular integral equation (33) for the temperature discontinuity density combined with Eq. (37) can be solved numerically (Erdogan and Gupta, 1972). Since the solution for the functions, $T_0(\xi)$, has a square root singular at both crack tips, it is more efficient for the numerical calculations by letting

$$T_0(\xi) = \frac{\Theta(\xi)}{\sqrt{c^2-\xi^2}} \tag{38}$$

where $\Theta(\xi)$ is a regular function defined in a closed interval $|\xi| \le c$. Once the function $\Theta(\xi)$ has been found, the corresponding SED can be given from Eqs. (1f) and (29) in the form

$$\Pi_1(\eta) = -\frac{1}{2\pi}\int_{-c}^{c} \mathrm{Im}\Big\{ -\mathbf{B}\mathbf{P}\Big[\mathbf{F}_{*1}'(z) + \mathbf{F}_{*2}'(z)\mathbf{P}^{-1}\bar{\tau}\Big]\mathbf{B}^{-1}\bar{\mathbf{d}} + \tau\mathbf{d}g_*'(z_t)\Big\} T_0(\xi)\,\mathrm{d}\xi \tag{39}$$

$$\Pi_2(\eta) = \frac{1}{2\pi}\int_{-c}^{c} \mathrm{Im}\Big\{ -\mathbf{B}\Big[\mathbf{F}_{*1}'(\mathbf{z}) + \mathbf{F}_{*2}'(\mathbf{z})\mathbf{P}^{-1}\bar{\tau}\Big]\mathbf{B}^{-1}\bar{\mathbf{d}} + \tau\mathbf{d}g_*'(z_t)\Big\} T_0(\xi)\,\mathrm{d}\xi \tag{40}$$

where

$$\mathbf{P} = \mathrm{diag}\big[\, p_1 \quad p_2 \quad p_3 \quad p_4 \,\big] \tag{41}$$

$$\mathbf{F}_{*i}(\mathbf{z}) = \mathrm{diag}\big[\, f_{*i}(z_1) \quad f_{*i}(z_2) \quad f_{*i}(z_3) \quad f_{*i}(z_4) \,\big], \quad i = 1, 2 \tag{42}$$

$$\begin{aligned}
f_{*i}(z_k) &= a\Big[F_1\big(\zeta_k, \zeta_t^*\big) + F_2\big(\zeta_k, \zeta_t^*\big) - F_1\Big(\zeta_k^{-1}, \bar{\zeta}_t^*\Big) - F_2\Big(\zeta_k^{-1}, \bar{\zeta}_t^*\Big)\Big]/2 \\
&+ e_{j1}a\gamma\Big[F_3\big(\zeta_k, \zeta_t^*\big) + F_4\big(\zeta_k, \zeta_t^*\big) - F_3\Big(\zeta_k^{-1}, \bar{\zeta}_t^*\Big) - F_4\Big(\zeta_k^{-1}, \zeta_t^*\Big)\Big]/2, \\
f_{*2}(z_k) &= ip_k a e\Big[-F_1\big(\zeta_k, \zeta_t^*\big) + F_2\big(\zeta_k, \zeta_t^*\big) - F_1\Big(\zeta_k^{-1}, \bar{\zeta}_t^*\Big) + F_2\Big(\zeta_k^{-1}, \bar{\zeta}_t^*\Big)\Big]/2 \\
&+ ie_{j1}p_k a e\gamma\Big[F_3\big(\zeta_k, \zeta_t^*\big) - F_4\big(\zeta_k, \zeta_t^*\big) + F_3\Big(\zeta_k^{-1}, \bar{\zeta}_t^*\Big) - F_4\Big(\zeta_k^{-1}, \bar{\zeta}_t^*\Big)\Big]/2
\end{aligned} \tag{43}$$

$$\begin{aligned}
g_*(z_t) &= a_{1\tau}\Big[F_1\big(\zeta_t, \zeta_t^*\big) - F_2\Big(\zeta_t^{-1}, \bar{\zeta}_t^*\Big)\Big] + a_{2\tau}\Big[F_2\big(\zeta_t, \zeta_t^*\big) - F_1\Big(\zeta_t^{-1}, \bar{\zeta}_t^*\Big)\Big] \\
&+ e_{j1}a_{3\tau}\Big[F_3\big(\zeta_t, \zeta_t^*\big) - F_4\Big(\zeta_t^{-1}, \bar{\zeta}_t^*\Big)\Big] + a_{4\tau}\Big[F_4\big(\zeta_t, \zeta_t^*\big) - F_3\Big(\zeta_t^{-1}, \bar{\zeta}_t^*\Big)\Big]
\end{aligned} \tag{44}$$

Thus the traction-charge vector on the crack faces is of the form

$$\mathbf{t}_0^n(\eta) = -\Pi_1(\eta)\sin\alpha + \Pi_2(\eta)\cos\alpha \tag{45}$$

It is, generally, that $\mathbf{t}_0^n(\eta)\neq 0$ on the crack faces $|\eta|\leq c$. To satisfy the traction-charge free condition (30b) on the crack faces, we must superpose a solution of the corresponding isothermal problem with a traction-charge vector equal and opposite to that of Eq. (45) in the range $|\eta|\leq c$. The electroelastic solution for a single dislocation of strength $\mathbf{b}_0$ in an infinite plate with a hole is thus required. This solution can be developed in a way similar to that given in Section 3.1. By applying the conformal mapping mentioned above and the perturbation concept (Stagni, 1982), the general electroelastic solution for the hole problem can be expressed as (Hwu and Yen, 1993)

$$\mathbf{u} = 2\mathrm{Re}\big[\mathbf{A}\mathbf{f}_0(\zeta) + \mathbf{A}\mathbf{f}_1(\zeta)\big] \tag{46}$$

$$\boldsymbol{\phi} = 2\mathrm{Re}\big[\mathbf{B}\mathbf{f}_0(\zeta) + \mathbf{B}\mathbf{f}_1(\zeta)\big] \tag{47}$$

in which the one-complex-variable approach introduced by Suo (1990) is adopted to make the derivation tractable. The approach stated that whether a function is analytic is not affected by different arguments ζ_k, and once a solution of $\mathbf{f}(\zeta)$ is obtained, the argument ζ should be replaced by ζ_k, to compute the related fields. This approach allows the standard matrix algebra to be used in conjunction with the techniques of analytic functions of one variable, and thus by pass some complexities arising from the use of four complex variables. $\mathbf{f}_0$ represents the function associated with the unperturbed electroelastic field which is related to the solutions of homogeneous media, $\mathbf{f}_1$ the function corresponding to the perturbed field of the matrix.

For a infinite plate subject to a line dislocation $\mathbf{b}_0$ located at $\hat{z}_k$, or ζ_k^* the function $\mathbf{f}_0$ can be assumed in the form (see Ting, 1992)

$$\mathbf{f}_0(\zeta) = \big\langle \ln\big(\zeta_k - \zeta_k^*\big)\big\rangle \mathbf{q}_0 \tag{48}$$

where $\langle(\,)_k\rangle = \mathrm{diag}[(\,)_1 \quad (\,)_2 \quad (\,)_3 \quad (\,)_4]$ and $\mathbf{q}_0$ can be determined by the condition (Ting, 1992)

$$\int_c \mathrm{d}\mathbf{u} = \mathbf{b}_0 \quad \text{for any closed curve } C \text{ enclosing the point } \zeta_k^* \tag{49}$$

Substitution of Eq. (48) into Eq. (49), yields

$$\mathbf{q}_0 = \frac{\mathbf{B}^{\mathrm{T}}\mathbf{b}_0}{2\pi i} \tag{50}$$

Thus the traction free condition on the hole boundary provides

$$\bar{\mathbf{B}}\,\overline{\mathbf{f}_0(\mathrm{e}^{i\psi})} + \mathbf{B}\mathbf{f}_1(\mathrm{e}^{i\psi}) = -\mathbf{B}\mathbf{f}_0(\mathrm{e}^{i\psi}) - \bar{\mathbf{B}}\,\overline{\mathbf{f}_1(\mathrm{e}^{i\psi})} \tag{51}$$

By the method of analytic continuation one sees (Hwu and Yen, 1993)

$$\mathbf{f}_1(\zeta) = -\mathbf{B}^{-1}\bar{\mathbf{B}}\,\overline{\mathbf{f}_0\big(1/\bar{\zeta}\big)} \tag{52}$$

The function $\mathbf{f}_1(\zeta)$ can be written explicitly in terms of ζ_k by substituting Eq. (48) into Eq. (52) with the understanding that the subscript of ζ is dropped before the multiplication of matrices and a replacement of ζ_k should be made for each component function of $\mathbf{f}_1(\zeta)$ after the multiplication of matrices. This results in (Hwu and Yen, 1993)

$$\mathbf{f}_1(\zeta) = \frac{\sum_{\beta=1}^{4}\left\langle \ln\left(\zeta_k^{-1} - \bar{\zeta}_\beta^*\right)\right\rangle \mathbf{B}^{-1}\bar{\mathbf{B}}\mathbf{I}_\beta\bar{\mathbf{B}}^{\mathrm{T}} b_0}{2\pi i} \tag{53}$$

where $\mathbf{I}_\beta = \mathrm{diag}[\,\delta_{1\beta} \quad \delta_{2\beta} \quad \delta_{3\beta} \quad \delta_{4\beta}\,]$, $\delta_{ij} = 1$ for $i = j$; $\delta_{ij} = 0$ for $i \neq j$.

Using Eqs. (45), (48) and (53), the boundary condition (31) can be expressed by (Qin, 1998)

$$\frac{\mathbf{L}}{2\pi}\int_{-c}^{c} \frac{\mathbf{b}_0(\xi)\,\mathrm{d}\xi}{\eta - \xi} + \frac{1}{\pi}\int_{-c}^{c} \mathbf{K}_0(\eta, \xi)\mathbf{b}_0(\xi)\,\mathrm{d}\xi = -\mathbf{t}_n^0(\eta) \tag{54}$$

where

$$\mathbf{L} = -2i\mathbf{B}\mathbf{B}^{\mathrm{T}} \tag{55}$$

$$K_0(\eta, \xi) = -\mathrm{Im}\left\{ \mathbf{B}\left\langle z_k^* \frac{\partial z_{kp}/\partial\zeta_k}{z_{kp}} \frac{\partial\zeta_k}{\partial z_k}\right\rangle \mathbf{B}^{\mathrm{T}} + \sum_{\beta=1}^{4} \mathbf{B}\left\langle \frac{z_k^*}{\zeta_k\left(1 - \zeta_k\bar{\zeta}_k^*\right)} \frac{\partial\zeta_k}{\partial z_k}\right\rangle \mathbf{B}^{-1}\bar{\mathbf{B}} I_\beta \bar{\mathbf{B}}^{\mathrm{T}} \right\} \tag{56}$$

and z_j^*, η and ξ are defined by

$$z_j^* = \cos\alpha + p_j \sin\alpha, \quad z_j = \eta z_j^* + z_j^0, \quad \hat{z}_\beta = \xi z_\beta^* + z_\beta^0 \tag{57}$$

$$z_{kp} = a_{1k} - \frac{a_{2k}}{\zeta_k\zeta_k^*} + \left(a_{3k} - \frac{a_{4k}}{\zeta_k^m\zeta_k^{*m}}\right)\sum_{j=0}^{m-1} \zeta_k^j \zeta_k^{*m-j-1} \tag{58}$$

where $\mathbf{L}$ is a real matrix, and $\mathbf{K}_0(\eta, \xi)$ is a kernel function of the singular integral equations and is Holder-continuous along $-c \le \xi \le c$.

For single valued displacements and electric potential around a closed contour surrounding the whole crack, the following conditions have also to be satisfied

$$\int_{-c}^{c} \mathbf{b}_0(\xi)\,\mathrm{d}\xi = 0 \tag{59}$$

As was done previously, let

$$\mathbf{b}_0(\xi) = \frac{\boldsymbol{\Theta}(\xi)}{\sqrt{c^2 - \xi^2}} \tag{60}$$

Once the function $\Theta(\xi)$ has been found from Eqs. (54) and (59), the stresses and electric displacements, $\boldsymbol{\Pi}_n(\eta)$, in a coordinate system local to the crack line can be expressed in the form

$$\boldsymbol{\Pi}_n(\eta) = \boldsymbol{\Omega}(\alpha)\left\{ \frac{\mathbf{L}}{2\pi}\int_{-c}^{c} \frac{\mathbf{b}_0(\xi)\,\mathrm{d}\xi}{\eta - \xi} + \frac{1}{\pi}\int_{-c}^{c} \mathbf{K}_0(\eta, \xi)\mathbf{b}_0(\xi)\,\mathrm{d}\xi + \mathbf{t}_n^0(\eta)\right\} \tag{61}$$

where the 4×4 matrix $\boldsymbol{\Omega}(\alpha)$ whose components are the cosine of the angle between the local coordinates and the global coordinates is in the form (Qin, 1998)

$$\boldsymbol{\Omega}(\alpha) = \begin{bmatrix} \cos\alpha & \sin\alpha & 0 & 0 \\ -\sin\alpha & \cos\alpha & 0 & 0 \\ 0 & 0 & 1 & 0 \\ 0 & 0 & 0 & 1 \end{bmatrix} \tag{62}$$

Using Eq. (61) we can evaluate the stress intensity factors $\mathbf{K}^* = (K_{II}, K_I, K_{III}, K_D)^{\mathrm{T}}$ at the tips, e.g., at the right tip ($\xi = c$) of the crack by following definition:

$$\mathbf{K}^* = \lim_{\xi \to c} + \sqrt{2\pi(\xi - c)}\boldsymbol{\Pi}_n(\xi) \tag{63}$$

Combined with the results of Eq. (61), one then leads to

$$\mathbf{K}^* \approx \sqrt{\frac{\pi}{4c}}\boldsymbol{\Omega}(\alpha)\mathbf{L}\boldsymbol{\Theta}(c) \tag{64}$$

Thus, the solution of the singular integral equation enables the direct determination of the stress intensity factors.

5. Numerical examples

As a numerical illustration of the proposed method, two simple examples are considered. One is a piezoelectric ceramic ($BaTiO_3$) plate with a crack of length $2c$ and a square hole, and another is an infinite isotropic elastic plate containing a circular and a crack. The purpose we consider the second example is for comparison with the existing results.

5.1. Example 1

Consider a piezoelectric ceramic ($BaTiO_3$) plate with a crack of length $2c$ and a square hole shown in Fig. 2, in which $x_{10} = 0$, $x_{20} = 3c$, $m = 3$, $e = 1$, $a = 1.8c$ and $\gamma = 0.2c$. The material properties of the plate are given by Qin and Mai (1998):

$$c_{11} = 150\ \text{GPa}, \quad c_{12} = 66\ \text{GPa}, \quad c_{13} = 66\ \text{GPa}, \quad c_{33} = 146\ \text{GPa}, \quad c_{44} = 44\ \text{GPa},$$

$$\alpha_{11} = 8.53 \times 10^{-6}/\text{K}, \quad \alpha_{33} = 1.99 \times 10^{-6}/\text{K}, \quad \lambda_3 = 0.133 \times 10^5\ \text{N/CK},$$

$$e_{31} = -4.35\ \text{C/m}^2, \quad e_{33} = 17.5\ \text{C/m}^2, \quad e_{15} = 11.4\ \text{C/m}^2, \quad \kappa_{11} = 1115\kappa_0,$$

$$\kappa_{33} = 1260\kappa_0, \quad \kappa_0 = 8.85 \times 10^{-12}\ \text{C}^2/\text{Nm}^2 = \text{Perimitivity of free space} \tag{65}$$

where c_{ij}, e_{ij} and k_{ij}, respectively, are the elastic moduli, piezoelectric constants and dielectric constants, α_{11} and α_{33} are thermal expansion constants, and λ_3 is a pyroelectric constant.

Since the values of the coefficient of heat conduction for $BaTiO_3$ could not be found in the literature, the value $k_{22}/k_{11} = 1.5$, $k_{12} = 0$ and $k_{11} = 1$ W/mK are assumed. Moreover, the plane strain deformation is assumed in our analysis and the crack lines are assumed to be in the x_1–x_2 plane, i.e., $D_3 = u_3 = 0$. Therefore the stress intensity factor vector $\mathbf{K}$ now has only three components(K_{II}, K_I, K_D). Fig. 3 shows the numerical results for the coefficients of stress intensity factors β_i versus the crack orientation α, where β_i, are defined by

$$K_I(A) = h_{20}c\sqrt{\pi c}\gamma_{33}\beta_1(\alpha)/k$$

$$K_{II}(A) = h_{20}c\sqrt{\pi c}\gamma_{11}\beta_2(\alpha)/k$$

$$K_D(A) = h_{20}c\sqrt{\pi c}\chi_3\beta_D(\alpha)/k \tag{66}$$

where

$$\begin{Bmatrix} \gamma_{11} \\ \gamma_{33} \\ \chi_3 \end{Bmatrix} = \begin{bmatrix} c_{11} & c_{13} & e_{31} \\ c_{13} & c_{33} & e_{33} \\ e_{31} & e_{33} & -\kappa_{33} \end{bmatrix} \begin{Bmatrix} \alpha_{11} \\ \alpha_{33} \\ \lambda_3 \end{Bmatrix} \tag{67}$$

However, numerical results for such a problem are not available in the literature yet. For comparison, the well-known finite element method (FEM) is used to obtain the corresponding results (Oden and Kelley, 1971). In the FEM analysis, four meshes ($M \times N$, 48×40, 72×60, 96×80, 120×100, where M and N are the element number on the side AB and side BC shown in Fig. 4) have been used to show the convergence of the FE results. For illustration, Fig. 4 shows the configuration of a particular element mesh ($M = 48$, $N = 40$ and $\alpha = 45^\circ$). Moreover, In order to accurately calculate the SED distribution at the crack tip, the mesh density has been increased near the crack tip. A typical finite element mesh ($\alpha = 45^\circ$) near crack tip is shown in Fig. 4(b). In the calculation, an eight-node quadrilateral element model has been used. In addition, the three nodes along one of the sides of each of the quadrilateral element are collapsed at the crack tip and the two adjoining mid points are moved to the quarter distances, in order to produce $1/r^{1/2}$ type of singularity. Table 4 shows that the FE results can converge to a particular value along with the mesh refinement. It can be seen from Fig. 3 that all the coefficients β_i,($i = 1, 2, D$) are not very sensitive to the crack orientation α, but slightly vary with it. It is also found from Fig. 3 that the numerical results obtained from the two models(FEM and proposed method) are in good agreement.

Further, to study the effects of mapping points on the numerical results, the calculation for SED intensity factors versus crack orientation α with different value of ζ_k (see section Section 2.2) has been carried out and the results are presented in Fig. 5, where line $|\zeta_{k1}| > |\zeta_{k2}| > |\zeta_{k3}| > |\zeta_{k4}|$. It is found from

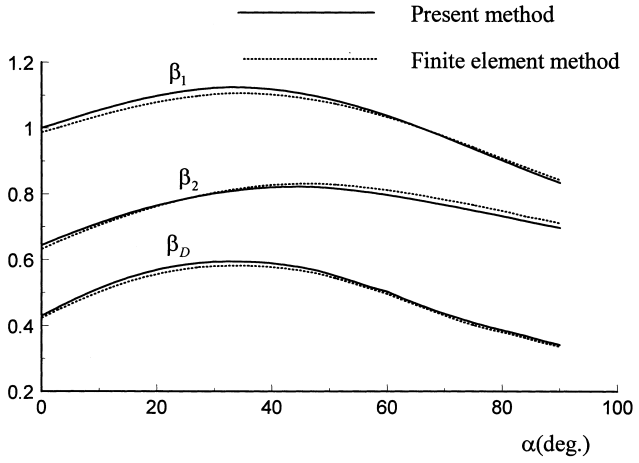

Fig. 3. Coefficients $\beta_i(i = 1, 2, D)$ vs. crack angle $\alpha M = 120$, $N = 100$).

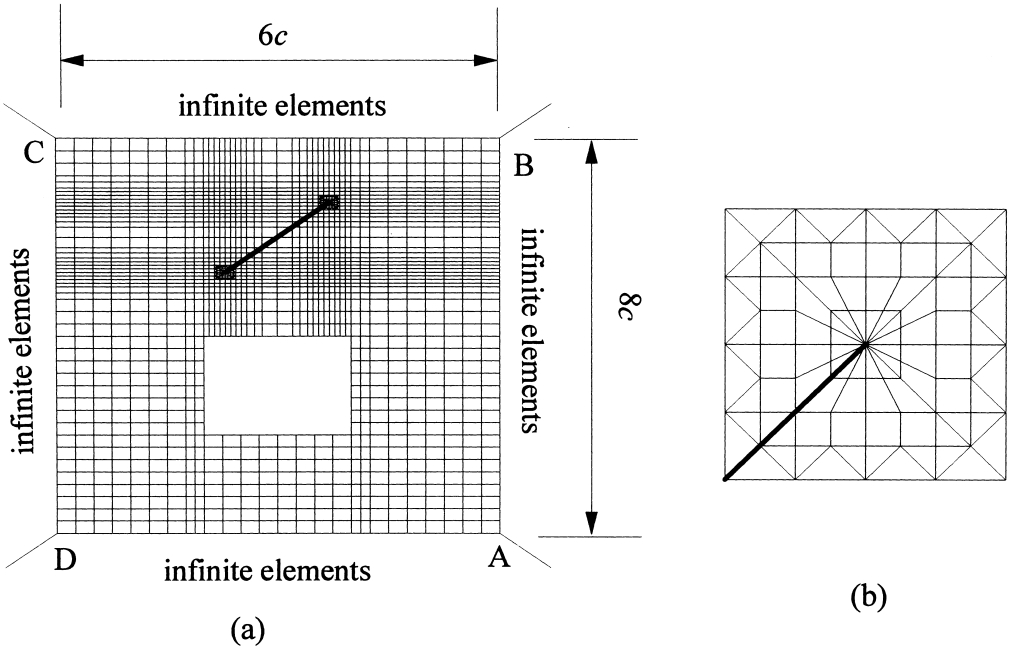

Fig. 4. (a) A typical mesh for element analysis ($M = 48$, $N = 40$), (b) mesh near crack tip.

Fig. 5 that the proposed formulation can give results consistent with those from FEM (in the FE calculation, the mesh $M \times N = 120 \times 100$ has been used) if we chose ζ_{k1} as the solution for Eq. (4), while other values of ζ_k produce unacceptable results.

5.2. Example 2

Consider a two-dimensional, linear, isotropic, thermoelastic plate which occupies the (r, θ) plane and contains a circular hole $0 \le r \le a$, $0 \le \theta \le 2\pi$, with a radial edge crack of length c on the line $\theta = 0$. The plate is subjected to a uniform heat flow h_0 as shown in Fig. 6. The problem was discussed by Hasebe et al. (1988) and can be treated as a degenerated case of the thermopiezoelectric problem. Fig. 7 shows the variation of normalized stress intensity factors(β_1 for $\theta_0 = 0^\circ$ and β_2 for $\theta_0 = 90^\circ$) with the ratio c/a and comparison is made with those given in (Hasebe et al., 1988). The coefficients β_i are defined as

Table 4
FE results versus mesh refinement ($\alpha = 0$)

Mesh ($M \times N$)	β_1	β_2	β_D
48×40	0.9687	0.6203	0.4085
72×60	0.9783	0.6271	0.4168
96×80	0.9848	0.6308	0.4210
120×100	0.9870	0.6321	0.4221

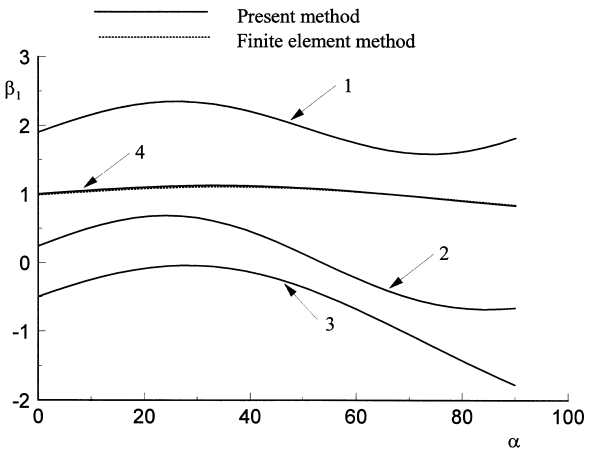

Fig. 5. Coefficients β_1 vs. crack angle α (1-with ζ_1, 2-with ζ_2, 3-with ζ_3, 4-with ζ_4).

$$K_{I(II)} = \frac{1+\nu}{k}\alpha h_0 G\beta_{1(2)}\sqrt{\pi\left(a+\frac{c}{2}\right)^3} \tag{68}$$

where k is the thermal conductivity, α the coefficient of thermal expansion, G the shear modulus and ν Poisson's ratio. It can be seen from Fig. 7 that $\beta_1 \to 0$ for both $c/a \to 0$ and $c/a \to \infty$ as well as $\beta_2 \to 0$ for $c/a \to 0$ and $\beta_2 \to 0.5$ for $c/a \to \infty$, which are in agreement with the analytical results (Hasebe et al., 1988).

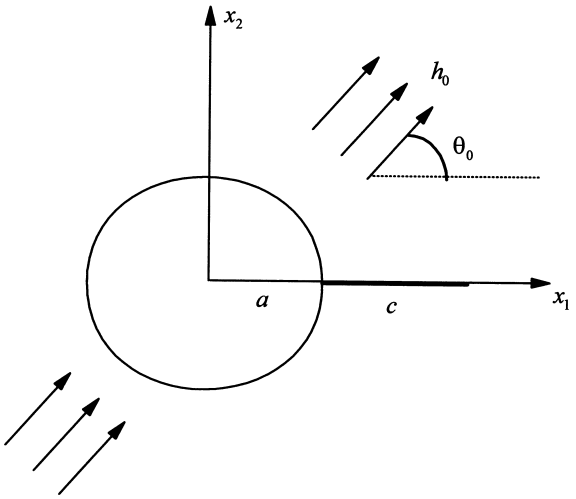

Fig. 6. Infinite region with a cracked circular hole under uniform heat flow.

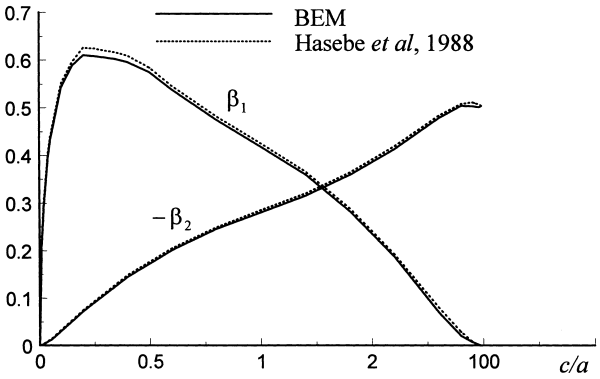

Fig. 7. Nondimensional stress intensity factors β_1 for $\theta_0 = 0^\circ$ and β_2 for $\theta_0 = 90^\circ$.

6. Conclusion

The general thermoelectroelastic solutions are presented for an infinite piezoelectric plate with various holes induced by thermal loads. The derivation is based on the Stroh formalism and the method of conformal mapping. The solutions satisfy traction-charge free as well as thermal-insulated conditions along the hole boundary. The key question for such a problem is that the transformation of a piezoelectric polygonal hole into a circle is not single-valued. In this paper, a simple approach is presented to treat this problem. Using the solutions developed here, a system of singular integral equations for the unknown temperature discontinuity defined on crack faces is developed to study the interaction between crack and hole. Numerical results of SED intensity factors for an infinite plate with one crack and a square hole are presented to illustrate the application of the proposed formulation. The numerical results show that an reasonable result can be obtained if we chose ξ_{k1}, whose magnitude has a minimum value among m-toots, as the solution for Eq. (4). The proposed method was further verified by the numerical comparison with the existing results (Hasebe et al., 1988).

Acknowledgements

The author wish to thank the Australian Research Council (ARC) for the continuing support of this work with a Queen Elizabeth II fellowship and the Australian Academy of Science by J.G. Russell Award. The comments and suggestions provided by anonymous reviewers of an earlier draft of this paper are also gratefully acknowledged.

References

Barnett, D.M., Lothe, J., 1975. Dislocations and line charges in anisotropic piezoelectric insulators. Phys. Stat. Sol. (b) 67, 105–111.

Chen, W.T., 1967. Plane thermal stress at an insulated hole under uniform heat flow in an orthotropic medium. J. Appl. Mech 34, 133–136.

Chung, M.Y., Ting, T.C.T., 1996. Piezoelectric solid with an elliptic inclusion or hole. Int. J. Solids Struct 33, 3343–3361.

Dhir, S.K., 1981. Optimization in a class of hole shapes in plate structures. J. Appl. Mech 48, 905–908.

Erdogan, F., Gupta, G.D., 1972. On the numerical solution of singular integral equations. Q. Appl. Math 32, 525–534.

Evan-Iwanowski, R.M., 1956. Stress solutions for an infinite plate with triangular Inlay. J. Appl. Mech 23, 336–338.
Florence, A.L., Goodier, J.N., 1960. Thermal stresses due to disturbance of uniform heat flow by an insulated Ovaloid hole. J. Appl. Mech 27, 635–639.
Gao, H., 1992. Stress analysis of holes in anisotropic elastic solids: conformal mapping and boundary perturbation. Q. J. Mech. Appl. Math 45, 149–168.
Hasebe, N., Tomida, A., Nakamura, T., 1988. Thermal stresses of a cracked circular hole due to uniform heat flux. J. Thermal Stresses 11 (1988), 381–391.
Hwu, C., 1990. Anisotropic plates with various openings under uniform loading or pure bending. J. Appl. Mech 57, 700–706.
Hwu, C., 1992. Polygonal holes in anisotropic media. Int. J. Solids & Struct 29, 2369–2384.
Hwu, C., Yen, W.J., 1991. Green's functions of two-dimensional anisotropic plates containing an elliptic hole. Int. J. Solids Struct 27, 1705–1719.
Hwu, C., Yen, W.J., 1993. On the anisotropic elastic inclusions in plane elastostatics. J. Appl. Mech 60, 626–632.
Jong, T.D., 1981. Stresses around rectangular holes in orthotropic plates. J. Comp. Mat 15, 311–328.
Kachanov, M., Tsukrov, I., Shafiro, B., 1994. Effective moduli of solids with cavities of various shapes. Appl. Mech. Rev 47 (1994), S151–S174.
Lekhnitskii, S.G., 1968. Anisotropic Plates. Gordon and Breach, London.
Mindlin, R.D., 1974. Equations of high frequency vibrations of thermopiezoelectric crystal plates. Int. J. Solids & Struct 10, 625–637.
Oden, J.T., Kelley, B.E., 1971. Finite element formulation of general electrothermoelasticity problems. Int. J. Numer. Meth. Eng 3, 161–179.
Qin, Q.H., 1998. Thermoelectroelastic Green's function for a piezoelectric plate containing an elliptic hole. Mechanics of Materials 30, 21–29.
Qin, Q.H., Mai, Y.W., Yu, S.W., 1999. Some problems in plane thermopiezoelectric materials with defects. Int. J. Solids Struc 36, 427–439.
Rajaiah, K., Naik, N.K., 1983. Optimum Quasi-rectangular holes in infinite orthotropic plates under in-plane loadings. J. Appl. Mech 50, 891–892.
Sosa, H., Khutoryansky, N., 1996. New developments concerning piezoelectric materials with defects. Int. J. Solids Struct 33, 3399–3414.
Stagni, L., 1982. On the elastic field perturbation by inhomogeneous in plane elasticity. ZAMP 33, 313–325.
Sturla, F.A., Barber, J.R., 1988. Thermal stresses due to a plane crack in general anisotropic material. J. Appl. Mech 55, 372–376.
Suo, Z., 1990. Singularities, interfaces and cracks in dissimilar anisotropic media. Proc. R. Soc. Lond A427, 331–358.
Ting, T.C.T., 1992. Image singularities of Green's functions for anisotropic elastic half-space and bimaterials. Q. J. Mech. Appl. Math 45, 119–139.
Ting, T.C.T., 1996. Green's functions for an anisotropic elliptic inclusion under generalized plane strain deformations. Q. J. Mech. Appl. Math 49, 1–18.
Wang, Y.M., Tarn, J.Q., 1993. Green's functions for generalized plane problems of anisotropic bodies with a hole or a rigid inclusion. J. Appl. Mech 60, 583–588.
Yen, W.J., Hwu, C., Liang, Y.K., 1995. Dislocation inside, outside or on the interface of an anisotropic elliptical inclusion. J. Appl. Mech 62 (1995), 306–311.
Zimmerman, R.W., 1986. Compressibility of two-dimensional cavities of various shapes. J. Appl. Mech 53, 500–504.